AMO - Advanced Modeling and Optimization, Volume 18, Number 2, 2016

SORET AND DUFOUR EFFECTS ON AN UNSTEADY MHD FREE CONVECTION FLOW PAST VERTICAL INCLINED HEATED PLATE EMBEDDED IN POROUS MEDIUM WITH THERMAL RADIATION

*MURALI GUNDAGANI
Department of Mathematics,
KG Reddy College of Engineering and Technology, India.

N.V.N BABU, AJIT PAUL
Department of Mathematics,SHIATS University,Allahabad,India.

Abstract: *In this analysis, the effects of Soret and Dufour have been discussed on unsteady MHD free convection heat and mass transfer flow on a viscous, incompressible, electrically conducting fluid past a semi – infinite inclined vertical porous plate, moving with a uniform velocity with chemical reaction and thermal radiation absorption. The chemical reaction has been assumed to be of first – order. The non – linear partial differential equations governing the flow have been solved numerically using finite difference method. Graphical results for velocity, temperature and concentration profiles have been obtained, to show the effects of different parameters entering in the problem. Such flow problems are important in many processes, in which there is combined heat and mass transfer with chemical reaction, such as drying, evaporation at the surface of water body etc.*

Keywords: *Soret, Dufour, Thermal radiation, MHD, Porous medium and Finite difference method.*

1. Introduction

The problems of free convective MHD flows are of prime importance in a number of industrial applications in Geo – physical and Astro – Physical situations. The problem of convective MHD flows has wide range of publications in emerging fields viz granular insulation, geothermal systems in heating and cooling chambers, fossil fuel, combustion, energy process, solar energy and space vehicle re entry. Some examples in living organisms are fluid transport mechanism among which the blood flow in circulatory system, with flow in airways. A classical example is in nuclear power station where the separation of uranium U_{235} from U_{238} by gases diffusion takes place. When heat and mass transfer occur simultaneously between the fluxes, the driving potentials are of more intricate nature.

*Corresponding Author:gundaganimurali@gmail.com

An energy flux can be generated not only by temperature gradients but also by composition gradients as well. The energy flux caused by a composition gradient is called Dufour or diffusion thermo effect. Temperature gradients can also create mass fluxes, and this is the Soret or thermal diffusion effect. Generally, the thermal diffusion and the diffusion thermo effects are of smaller order magnitude than the effects prescribed by Fourier's or Fick's laws and are often neglected in heat and mass transfer processes. However, there are exceptions. The thermal diffusion effect, for instance, has been utilized for isotope separation and in mixture between gases with very light molecular weight (Hydrogen – Helium) and of medium molecular weight (Nitrogen – Air) the diffusion thermo effect was found to be of a magnitude such that it cannot be neglected. In recent years, progress has been considerably made in the study of heat and mass transfer in magnetohydrodynamic flows due to its application in many devices. Afify [1] carried out an analysis to study free convective heat and mass transfer of an incompressible, electrically conducting fluid over a stretching sheet in the presence of suction and injection with thermal diffusion and diffusion thermo effects. Alam *et al*. [2] studied numerically the Dufour and Soret effects on combined free – forced convection and mass transfer flow past a semi – infinite vertical plate under the influence of transversely applied magnetic field. Gaikwad *et al.* [3] investigated the onset of double diffusive convection in two component couple of stress fluid layer with Soret and Dufour effects using both linear and non – linear stability analysis. Hayat *et al*. [4] discussed the effects of Soret and Dufour on heat and mass transfer on mixed convection boundary layer flow over a stretching vertical surface in a porous medium filled with a viscoelastic fluid. Kafoussias *et al.* [5] considered the boundary layer – flows in the presence of Soret, and Dufour effects associated with the thermal diffusion and diffusion thermo for the mixed forced natural convection. Lyubinova *et al*. [6] deals with the numerical investigation of the influence of static and vibrational acceleration on the measurement of diffusion and Soret coefficients in binary mixtures, in low gravity conditions. Mansour *et al.* [7] investigated the effects of chemical reaction, thermal stratification, Soret and Dufour numbers on MHD free convective heat and mass transfer of a viscous, incompressible and electrically conducting fluid over a vertical stretching surface embedded in a saturated porous medium. Ming – chun *et al*. [8] studied Soret and Dufour effects in strongly endothermic chemical reaction system of porous media. Motsa [9] investigated the effects of Soret and Dufour numbers on the onset of double diffusive convection. Osalusi *et al*. [10] investigated thermo diffusion and diffusion thermo effects on combined heat and mass transfer of a steady hydromagnetic convective and slip flow due to a rotating disk in the presence of viscous dissipation and Ohmic heating.

The study of heat and mass transfer problems with chemical reaction are of great practical importance to engineers and scientists because of their almost universal occurrence in many branches of science and engineering. A few representative fields of interest in which combined heat and mass transfer along with chemical reaction play an important role in chemical process industries such as food processing and polymer production. Beg *et al.* [11] have also analyzed the chemical reaction rate effects on steady buoyancy – driven dissipative micropolar free convective heat and mass transfer in a Darcian porous regime. Effects of chemical reaction on free convection flow of a polar fluid through a porous medium in the presence of internal heat generation are examined by Patil and Kulkarni [12]. Seddeek *et al.* [13] more recently reported on the effect of chemical reaction and variable viscosity on hydromagnetic mixed convection heat and mass transfer for Hiemenz flow through a Darcian porous media in the presence of radiation and magnetic field. Zueco *et al.* [14] recently examined the influence of chemical reaction on the hydromagnetic heat and mass transfer boundary layer flow from a horizontal cylinder in a Darcy – Forchheimer regime using network simulation. Gireesh Kumar *et al.* [15] investigated effects of chemical reaction and mass transfer on MHD unsteady free convection flow past an infinite vertical plate with constant suction and heat sink. Ibrahim [16] studied the effects of chemical reaction and radiation absorption on transient hydromagnetic natural convection flow with wall transpiration and heat source.

Motivated by the above reference work and the numerous possible industrial applications of the problem (like in isotope separation), it is of paramount interest in this study to investigate the effects Soret and Dufour on unsteady MHD free convection heat and mass transfer flow on a viscous, incompressible, electrically conducting fluid past a semi – infinite inclined vertical porous plate, moving with a uniform velocity with chemical reaction and thermal radiation absorption. Hence, the objective of this paper is to study the more general problem which includes the Soret and Dufour effects on an unsteady MHD flow and heat transfer along a porous flat plate with mass transfer in presence of viscous dissipation and chemical reaction. In this study, the effects of different flow parameters encountered in the equations are also studied. The problem is solved numerically using the finite difference method, which is more economical from the computational view point.

2.Mathematical formulation:

Consider a two – dimensional unsteady MHD free convection flow of a viscous, incompressible, electrically conducting fluid past a semi – infinite tilted porous plate with chemical reaction and thermal radiation. In Cartesian coordinate system, let $x'-$axis is taken to be along the plate and the $y'-$axis normal to the plate. Since the plate is considered infinite in $x'-$direction, hence all physical quantities will be independent of $x'-$direction. The wall is maintained at constant temperature (T'_w) and concentration (C'_w) higher than the ambient temperature (T'_∞) and concentration (C'_∞) respectively. A uniform magnetic field of magnitude B_o is applied normal to the plate. The transverse applied magnetic field and magnetic Reynold's number are assumed to be very small, so that the induced magnetic field is negligible. Consider an unsteady magnetohydrodynamic free convection flow of a viscous, incompressible, electrically conducting fluid past a semi – infinite tilted porous plate with an angle α to the vertical. The homogeneous chemical reaction of first order with rate constant $\overline{K}$ between the diffusing species and the fluid is assumed. It is assumed that there is no applied voltage which implies the absence of an electric field. The fluid has constant kinematic viscosity and constant thermal conductivity, and the Boussinesq's approximation have been adopted for the flow. The fluid is considered to be gray absorbing – emitting radiation but non – scattering medium and the Roseland's approximation is used to describe the radiative heat flux. It is considered to be negligible in $x'-$direction as compared in $y'-$ direction. At time $t'>0$ the plate is given an impulsive motion in the direction of flow i.e. along $x'-$axis against the gravity with constant velocity U_o, it is assumed that the plate temperature and concentration at the plate are varying linearly with time. Under these assumptions the equations governing the flow are:

Momentum Equation:

$$\frac{\partial u'}{\partial t'} = g\beta(T'-T'_\infty)(\cos\alpha) + g\beta^*(C'-C'_\infty)(\cos\alpha) + \nu\frac{\partial^2 u'}{\partial y'^2} - \left(\frac{\sigma B_o^2}{\rho} + \frac{\nu}{K'}\right)u' \tag{1}$$

Energy Equation:

$$\rho C_p \frac{\partial T'}{\partial t'} = \kappa\frac{\partial^2 T'}{\partial y'^2} - \frac{\partial q_r}{\partial y'} + \nu\left(\frac{\partial u'}{\partial y'}\right)^2 + Q'(T'-T'_\infty) + \frac{D_m k_T}{C_S C_P}\frac{\partial^2 C'}{\partial y'^2} \tag{2}$$

Species Diffusion Equation:

$$\frac{\partial C'}{\partial t'} = D\frac{\partial^2 C'}{\partial y'^2} - K_r(C'-C'_\infty) + \frac{D_m k_T}{T_m}\frac{\partial^2 T'}{\partial y'^2} \tag{3}$$

With the following initial and boundary conditions:

$$\left.\begin{array}{l} t'\le 0: u'=0,\ T'=T'_\infty,\ C'=C'_\infty \quad for \quad all \quad y' \\ t'>0:\begin{cases} u'=U_o,\ T'=T'_\infty+(T'_w-T'_\infty)At',\ C'=C'_\infty+(C'_w-C'_\infty)At',\ at\ \ y'=0 \\ u'\to 0,\ T'\to 0,\ C'\to 0 \quad as \quad y'\to\infty \end{cases} \end{array}\right\} \tag{4}$$

Where $A=\frac{U_o^2}{\nu}$. The radiative heat flux q_r, under Rosseland approximation has the form

$$q_r = -\frac{4\sigma}{3\kappa}\frac{\partial^2 T'^4}{\partial y'} \tag{5}$$

It is assumed that, the temperature differences within the flow are sufficiently small such that T'^4 may be expressed as a linear function of the temperature T'_∞. This is obtained by expanding T'^4 in a Taylor series about T'_∞ and neglecting higher order terms.

Thus, we get $T'^4 \cong 4T'^3_\infty T' - 3T'^4_\infty$ (6)

By using equations (5) and (6), equation (2) reduces to

$$\frac{\partial T'}{\partial t'} = \frac{\kappa}{\rho C_p}\frac{\partial^2 T'}{\partial y'^2} - \frac{16\sigma T'^3_\infty}{3k_1 \rho C_p}\frac{\partial^2 T'}{\partial y'^2} \tag{7}$$

Introducing the following non – dimensional parameters in equations (1), (2), (3) and (7) quantities:

$$\left.\begin{aligned} & y = \frac{y'U_o}{\nu}, t = \frac{t'U_o}{\nu}, u = \frac{u'}{U_o}, \ \theta = \frac{T' - T'_\infty}{T'_w - T'_\infty}, \ C = \frac{C' - C'_\infty}{C'_w - C'_\infty}, Gr = \frac{g\beta\nu\left(T'_w - T'_\infty\right)}{U_o^3}, \ Sc = \frac{\nu}{D}, \\ & Gc = \frac{g\beta^*\nu\left(C'_w - C'_\infty\right)}{U_o^3}, \Pr = \frac{\mu C_p}{\kappa}, M = \left(\frac{\sigma B_o^2}{\rho}\right)\frac{\nu}{U_o^2}, Ec = \frac{U_o^2}{C_p\left(T'_w - T'_\infty\right)}, \ Q = \frac{\nu Q'}{\rho C_p U_o^2}, \\ & K = \frac{K'U_o^2}{\nu^2}, N = \frac{\kappa U_o^2}{4\nu^2\sigma T'^3_\infty}, \ k_r = \frac{K_r\nu}{U_o^2}, \ Du = \frac{D_m k_T (C'_w - C'_\infty)}{C_S C_P (T'_w - T'_\infty)}, \ Sr = \frac{D_m k_T (T'_w - T'_\infty)}{\nu T_m (C'_w - C'_\infty)} \end{aligned}\right\} \tag{8}$$

In equations (1), (2), (3) and (7) reduces to

$$\frac{\partial u}{\partial t} = \frac{\partial^2 u}{\partial y^2} - (M + \frac{1}{K})u + \left(Gr\right)(\cos\alpha)\theta + \left(Gc\right)(\cos\alpha)C \tag{9}$$

$$\left(\Pr\right)\frac{\partial \theta}{\partial t} = \left(1 + \frac{4}{3N}\right)\frac{\partial^2\theta}{\partial y^2} + (\Pr)(Ec)\left(\frac{\partial u}{\partial y}\right)^2 + \left(Du\right)\left(\Pr\right)\left(\frac{\partial^2 C}{\partial y^2}\right) - \left(\Pr\right)\left(Q\right)\theta \tag{10}$$

$$\frac{\partial C}{\partial t} = \frac{1}{Sc}\frac{\partial^2 C}{\partial y^2} + Sr\left(\frac{\partial^2\theta}{\partial y^2}\right) - \left(k_r\right)C \tag{11}$$

The corresponding initial and boundary conditions in dimensionless form are:

$$\left.\begin{aligned} & t \le 0: \ \ u = 0, \ \theta = 0, \ C = 0 \quad for \quad all \quad y \\ & t > 0: \begin{cases} u = 1, \ \theta = t, \ C = t \quad at \quad y = 0 \\ u \to 0, \quad \theta \to 0, \quad C \to 0 \quad as \quad y \to \infty \end{cases} \end{aligned}\right\} \tag{12}$$

All the physical parameters are defined in the nomenclature. It is now important to calculate the physical quantities of primary interest, which are the local wall shear stress, the local surface heat and mass flux. Given the velocity field in the boundary layer, we can now calculate the local wall shear stress (i.e., skin – friction) is given by and in dimensionless form, we obtain knowing the temperature field, it is interesting to study the effect of the free convection and radiation on the rate of heat transfer. This is given by which is written in dimensionless form as

$$\tau = \frac{\tau_w}{\rho u_w^2}, \quad \tau_w = \left[\mu \frac{\partial u}{\partial y}\right]_{y'=0} = \rho U_o^2 u'(0) = \left[\frac{\partial u}{\partial y}\right]_{y=0} \tag{13}$$

The dimensionless local surface heat flux (i.e., Nusselt number) is obtained as

$$N_u(x') = -\left[\frac{x'}{(T'_w - T'_\infty)} \frac{\partial T'}{\partial y'}\right]_{y'=0} \quad \text{then } Nu = \frac{N_u(x')}{R_{e_x}} = -\left[\frac{\partial \theta}{\partial y}\right]_{y=0} \tag{14}$$

The definition of the local mass flux and the local Sherwood number are respectively given by with the help of these equations, one can write

$$S_h(x') = -\left[\frac{x'}{(C'_w - C'_\infty)} \frac{\partial C'}{\partial y'}\right]_{y'=0} \quad \text{then } Sh = \frac{S_h(x')}{R_{e_x}} = -\left[\frac{\partial C}{\partial y}\right]_{y=0} \tag{15}$$

Where $R_{e_x} = -\frac{U_o x'}{\nu}$ is the Reynold's number.

The mathematical formulation of the problem is now completed. Equations (9) – (11) present a coupled non – linear system of partial differential equations and are to be solved by using initial and boundary conditions (12). However, exact solutions are difficult, whenever possible. Hence, these equations are solved by the Crank Nicholson method.

3.Method of Solution

We shall solve the system of partial differential equations numerically using the finite difference technique and equations (9) – (11) yield.

$$\left(\frac{u_i^{j+1} - u_i^j}{\Delta t}\right) = \left(\frac{u_{i+1}^j - 2u_i^j + u_{i-1}^j}{(\Delta y)^2}\right) - \left(M + \frac{1}{K}\right)u_i^j + (Gr)(\cos\alpha)\theta_i^j + (Gc)(\cos\alpha)C_i^j \tag{16}$$

$$(\Pr)\left(\frac{\theta_i^{j+1} - \theta_i^j}{\Delta t}\right) = \left(1 + \frac{4N}{3}\right)\left(\frac{\theta_{i+1}^j - 2\theta_i^j + \theta_{i-1}^j}{(\Delta y)^2}\right) + (\Pr)(Ec)\left(\frac{u_{i+1}^j - u_i^j}{\Delta y}\right)^2 + (\Pr)(Du)\left(\frac{C_{i+1}^j - 2C_i^j + C_{i-1}^j}{(\Delta y)^2}\right) - (\Pr)(Q)\theta_i^j \tag{17}$$

$$(Sc)\left(\frac{C_i^{j+1} - C_i^j}{\Delta t}\right) = \left(\frac{C_{i+1}^j - 2C_i^j + C_{i-1}^j}{(\Delta y)^2}\right) - (k_r)(Sc)C_i^j + (Sc)(Sr)\left(\frac{\theta_{i+1}^j - 2\theta_i^j + \theta_{i-1}^j}{(\Delta y)^2}\right) \tag{18}$$

Where the indices i and j refer to y and t respectively. The initial and boundary conditions (12) yields

$$\left.\begin{array}{l} t\le 0:\; u_i^j=0,\; \theta_i^j=0,\; C_i^j=0 \quad for\ all\ \ y \\ t>0:\begin{cases} u_i^j=1,\ \theta_i^j=t,\ C_i^j=t\ \ at\ \ y=0 \\ u_i^j\to 0,\ \theta_i^j\to 0,\ C_i^j\to 0\ \ as\ \ y\to\infty \end{cases} \end{array}\right\} \tag{19}$$

The term consistency applied to a finite difference procedure means that the procedure may in fact approximate the solution of the partial differential equation under study and not the solution of any other partial differential equation. The consistency is measured in terms of the difference between a differential equation and a difference equation. Here, we can write

$$\frac{\partial u}{\partial t}=\frac{u_i^{j+1}-u_i^j}{\Delta t}+O(\Delta t),\ \frac{\partial \theta}{\partial t}=\frac{\theta_i^{j+1}-\theta_i^j}{\Delta t}+O(\Delta t),\ \frac{\partial C}{\partial t}=\frac{C_i^{j+1}-C_i^j}{\Delta t}+O(\Delta t),$$

$$\frac{\partial^2 u}{\partial y^2}=\frac{u_{i+1}^j-2u_i^j+u_{i-1}^j}{(\Delta y)^2}+O(\Delta y)^2,\ \frac{\partial^2 \theta}{\partial y^2}=\frac{\theta_{i+1}^j-2\theta_i^j+\theta_{i-1}^j}{(\Delta y)^2}+O(\Delta y)^2\ \ \&\ \ \frac{\partial^2 C}{\partial y^2}=\frac{C_{i+1}^j-2C_i^j+C_{i-1}^j}{(\Delta y)^2}+O(\Delta y)^2$$

For consistency of equation (16), we estimate

$$\begin{aligned}&\left\{\left(\frac{u_i^{j+1}-u_i^n}{\Delta t}\right)-\left(\frac{u_{i+1}^j-2u_i^j+u_{i-1}^j}{(\Delta y)^2}\right)+\left(M+\frac{1}{K}\right)u_i^j-(Gr)(\cos\alpha)\theta_i^j-(Gc)(\cos\alpha)C_i^j\right\}\\&-\left\{\frac{\partial u}{\partial t}-\frac{\partial^2 u}{\partial y^2}+(M+\frac{1}{K})u-(Gr)(\cos\alpha)\theta-(Gc)(\cos\alpha)C\right\}_{i,\,j}=O(\Delta t)+O(\Delta y)^2\end{aligned} \tag{20}$$

For consistency of equation (17), we estimate

$$\begin{aligned}&\left\{(\Pr)\left(\frac{\theta_i^{j+1}-\theta_i^j}{\Delta t}\right)-\left(1+\frac{4N}{3}\right)\left(\frac{\theta_{i+1}^j-2\theta_i^j+\theta_{i-1}^j}{(\Delta y)^2}\right)-(\Pr)(Ec)\left(\frac{u_{i+1}^j-u_i^j}{\Delta y}\right)^2-(\Pr)(Du)\left(\frac{C_{i+1}^j-2C_i^j+C_{i-1}^j}{(\Delta y)^2}\right)+(\Pr)(Q)\theta_i^j\right\}\\&-\left\{(\Pr)\frac{\partial\theta}{\partial t}-\left(1+\frac{4}{3N}\right)\frac{\partial^2\theta}{\partial y^2}-(\Pr)(Ec)\left(\frac{\partial u}{\partial y}\right)^2-(Du)(\Pr)\left(\frac{\partial^2 C}{\partial y^2}\right)+(\Pr)(Q)\theta\right\}_{i,\,j}=O(\Delta t)+O(\Delta y)^2\end{aligned} \tag{21}$$

Similarly with respect to equation (18)

$$\begin{aligned}&\left\{(Sc)\left(\frac{C_i^{j+1}-C_i^j}{\Delta t}\right)-\left(\frac{C_{i+1}^j-2C_i^j+C_{i-1}^j}{(\Delta y)^2}\right)+(k_r)(Sc)C_i^j-(Sc)(Sr)\left(\frac{\theta_{i+1}^j-2\theta_i^j+\theta_{i-1}^j}{(\Delta y)^2}\right)\right\}\\&-\left\{(Sc)\frac{\partial C}{\partial t}-\frac{\partial^2 C}{\partial y^2}-(Sc)(Sr)\left(\frac{\partial^2\theta}{\partial y^2}\right)+(k_r)(Sc)C\right\}_{i,\,j}=O(\Delta t)+O(\Delta y)^2\end{aligned} \tag{22}$$

Here, the right hand side of equations (20) – (22) represents truncation error as $\Delta t\to 0$ with $(\Delta y)^2\to 0$, the truncation error tends to zero. Hence our explicit scheme is consistent. Here $(\Delta y)^2$, Δt are mesh sizes along y

and time direction respectively. The infinity taken as $i = 1$ to n and the equations (20), (21) and (22) are solved under the boundary conditions (19), following the tri diagonal system of equations are obtained.

$$A_i X_i = B_i \ (i = 1 \text{ to } n) \tag{23}$$

Where A_i is the tri diagonal matrix of order $n \times n$ and X_i, B_i are the column matrices having n components. The above system of equations has been solved by Thomas Algorithm (Gauss elimination method), for velocity, temperature and concentration. In order to prove the convergence of the finite difference scheme, the computations are carried out for different values of Δt. But the Crank – Nicholson method is unconditionally stable. By changing the value of Δt there is no change in the study state condition. So, the finite difference scheme is convergent and stable.

4. Results and Discussion

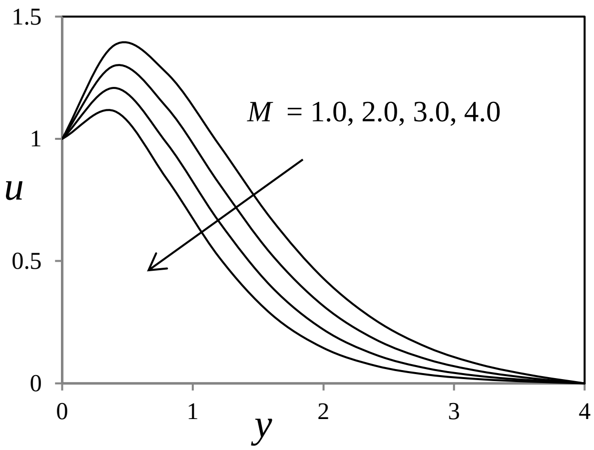

Figure 1. Velocity profiles for different values of Magnetic field (Hartmann number)

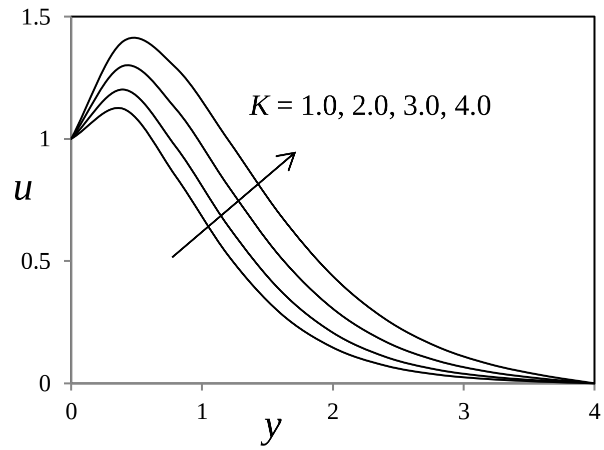

Figure 2. Velocity profiles for different values of Permeability parameter

In order to get a physical insight in to the problem the effects of various governing parameters on the physical quantities are computed and represented in figures (1) – (19) and discussed in detail. The effect of the Hartmann number (M) is shown in figure (1). It is observed that the velocity of the fluid decreases with the increase of the magnetic field number values. The decrease in the velocity as the Hartmann number (M) increases is because the presence of a magnetic field in an electrically conducting fluid introduces a force called the Lorentz force, which acts against the flow if the magnetic field is applied in the normal direction, as in the present study. This resistive force slows down the fluid velocity component as shown in figure (1).

The effect of Permeability parameter (K) on velocity is presented in the figure (2). From this figure we observe that, the fluid velocity increases with increase in the permeability parameter in the boundary layer region. The physics behind this phenomenon is that an increase in permeability parameter implies that there is a decrease in the resistance of porous medium, which tends to enhance the fluid flow.

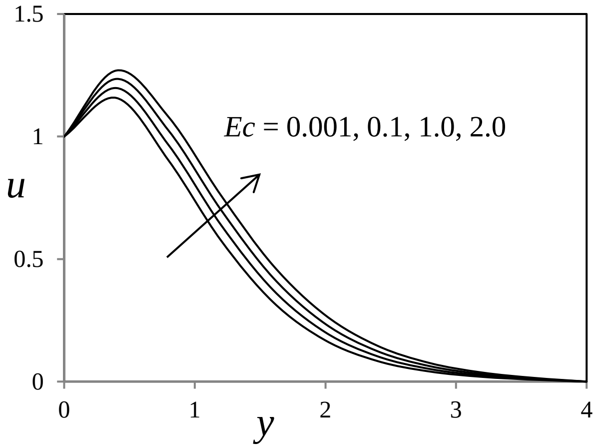

Figure 3. Velocity profiles for different values of Eckert number

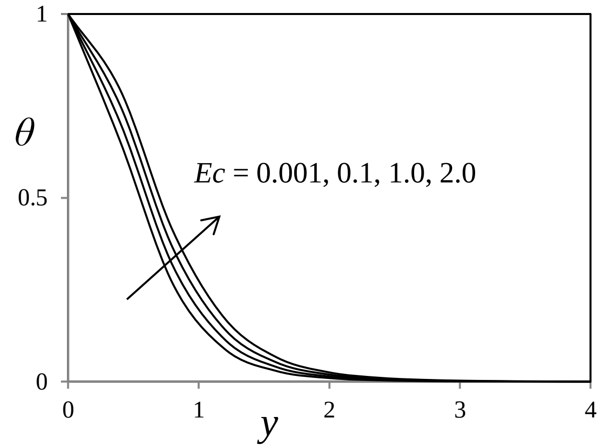

Figure 4. Temperature profiles for different values of Eckert number

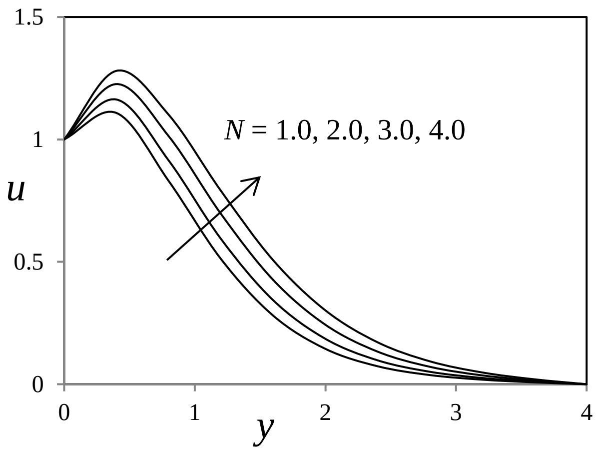

Figure 5. Velocity profiles for different values of Thermal radiation parameter

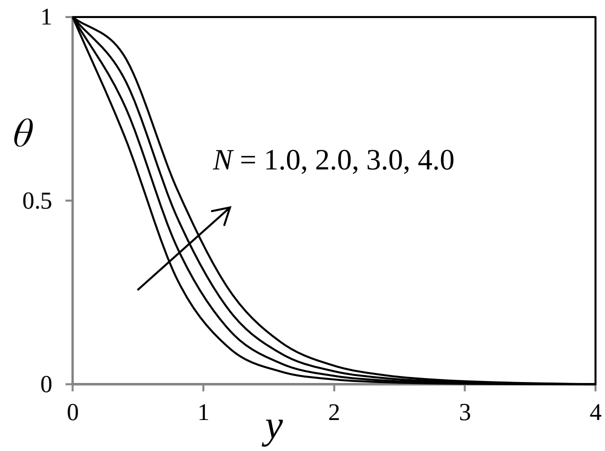

Figure 6. Temperature profiles for different values of Thermal radiation parameter

The influence of the viscous dissipation parameter i.e., the Eckert number on the velocity and temperature are shown in figures (3) and (4) respectively. The Eckert number expresses the relationship between the kinetic energy in the flow and the enthalpy. It embodies the conversion of kinetic energy into internal energy by work done against the viscous fluid stresses. Greater viscous dissipative heat causes a rise in the temperature as well as the velocity. This behavior is evident from figures (3) and (4). The effects of the thermal radiation parameter on the velocity and temperature profiles in the boundary layer are illustrated in figures (5) and (6) respectively. Increasing the thermal radiation parameter produces significant increase in the thermal condition of the fluid and its thermal boundary layer. This increase in the fluid temperature induces more flow in the boundary layer causing the velocity of the fluid there to increase.

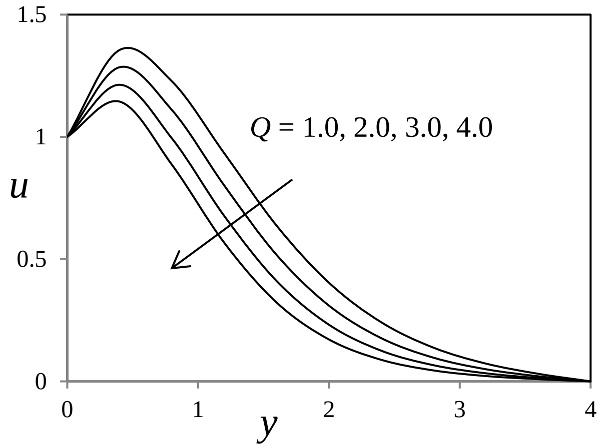

Figure 7. Velocity profiles for different values of Heat absorption parameter

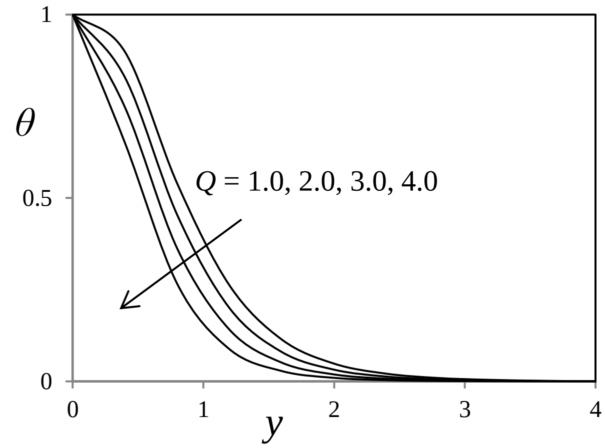

Figure 8. Temperature profiles for different values of Heat absorption parameter

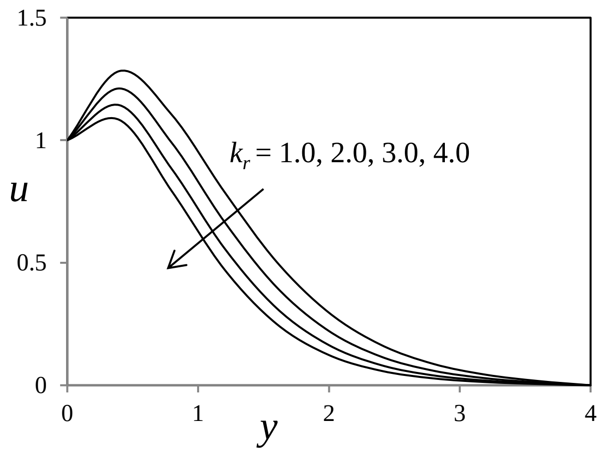

Figure 9. Velocity profiles for different values of Chemical reaction parameter

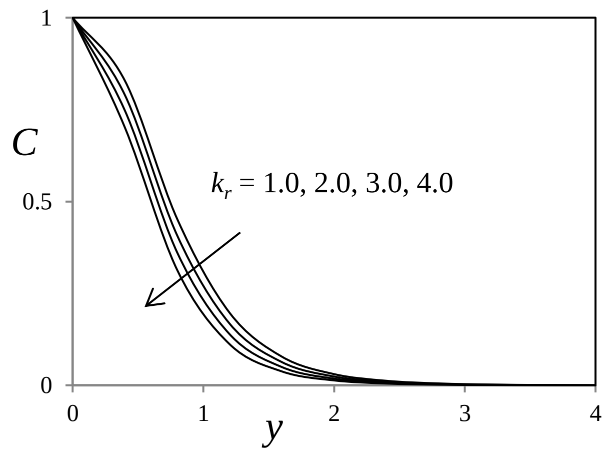

Figure 10. Concentration profiles for different values of Chemical reaction parameter

Figures (7) and (8) illustrate the influence of heat absorption coefficient (Q) on the velocity and temperature at t = 1.0 respectively. Physically speaking, the presence of heat absorption (thermal sink) effects has the tendency to reduce the fluid temperature. This causes the thermal buoyancy effects to decrease resulting in a net reduction in the fluid velocity. These behaviors are clearly obvious from figures (7) and (8) in which both the velocity and temperature distributions decrease as Q increases. It is also observed that the both the hydrodynamic (velocity) and the thermal (temperature) boundary layers decrease as the heat absorption effects increase. Figures (9) and (10) display the effects of the chemical reaction parameter on the velocity and concentration profiles, respectively. As expected, the presence of the chemical reaction significantly affects the concentration profiles as well as the velocity profiles. It should be mentioned that the studied case is for a destructive chemical reaction k_r. In fact, as chemical reaction increases, the considerable reduction in the velocity profiles is predicted, and the presence of the peak indicates that the maximum value of the velocity occurs in the body of the fluid close to the surface but not at the surface. Also, with an increase in the chemical reaction parameter, the concentration decreases. It is evident that the increase in the chemical reaction significantly alters the concentration boundary layer thickness but does not alter the momentum boundary layers.

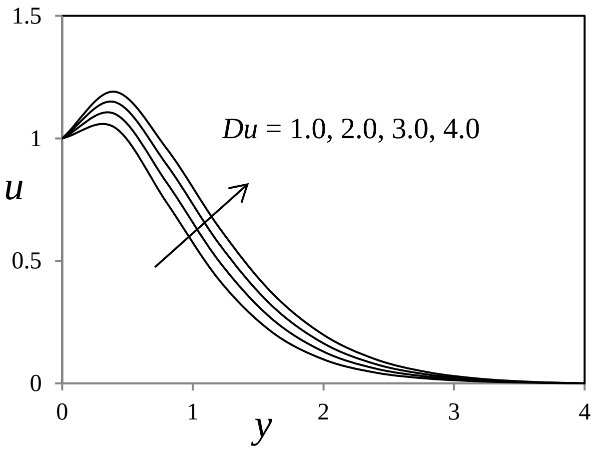

Figure 11. Velocity profiles for different values of Dufour number

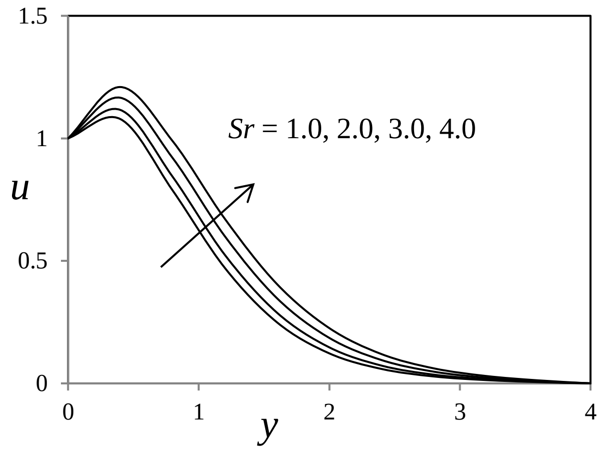

Figure 12. Velocity profiles for different values of Soret number

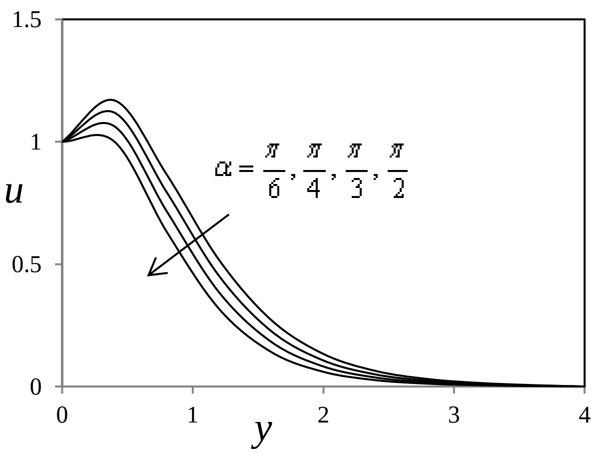

Figure 13. Velocity profiles for different values of Phase angle

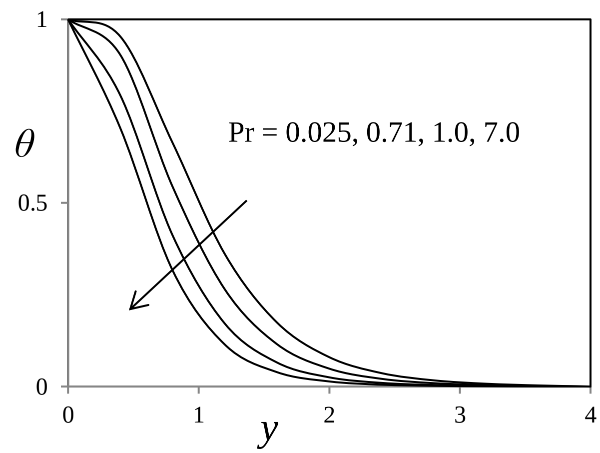

Figure 14. Temperature profiles for different values of Prandtl number

The variations of velocity distribution with y for different values of the Dufour number (Du) are shown in figure (11). In this figure, it can be clearly seen that as the Dufour number increases, the velocity increases. The variations of velocity distribution with y for different values of the Soret number (Sr) are shown in figure (12). It can be clearly seen that the velocity distribution in the boundary layer increases with the Soret number.

It is interesting note that the effect of Dufour and Soret numbers on velocity field are little significant. This is because either a decrease in concentration difference or an increase in temperature difference leads to an increase in the value of the Soret parameter (Sr). Hence increasing the Soret parameter (Sr) increases the velocity of the fluid. The effect of Phase angle (α) on the velocity field has been illustrated in figure (13). It is seen that as the Phase angle increases the velocity field decreases. In figure (14) we depict the effect of Prandtl number on the temperature field. It is observed that an increase in the Prandtl number leads to decrease in the temperature field. Also, temperature field falls more rapidly for water in comparison to air and the temperature curve is exactly linear for mercury, which is more sensible towards change in temperature. From this observation it is conclude that mercury is most effective for maintaining temperature differences and can be used efficiently in the laboratory. Air can replace mercury, the effectiveness of maintaining temperature changes are much less than mercury. However, air can be better and cheap replacement for industrial purpose. This is because, either increase of kinematic viscosity or decrease of thermal conductivity leads to increase in the value of Prandtl number. Hence temperature decreases with increasing of Prandtl number.

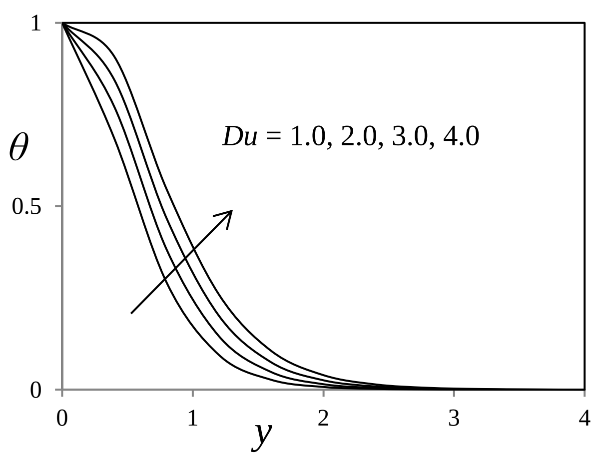

Figure 15. Temperature profiles for different values of Dufour number

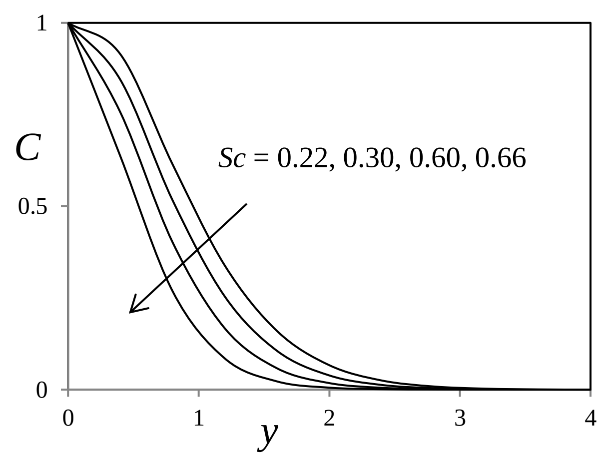

Figure 16. Concentration profiles for different values of Schmidt number

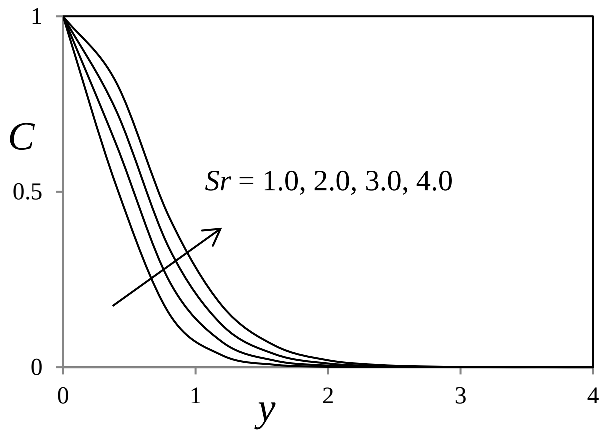

Figure 17. Concentration profiles for different values of Soret number

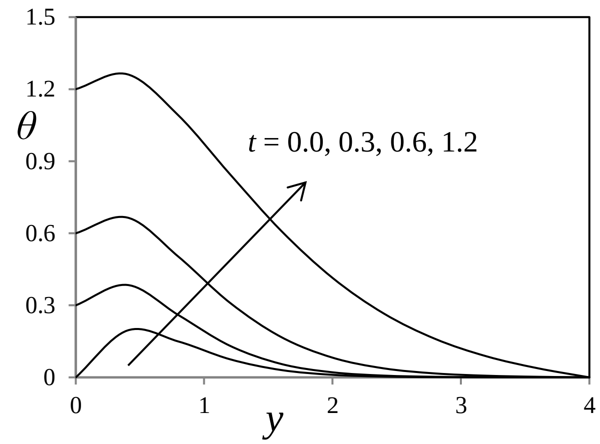

Figure 18. Temperature profiles for different values of time

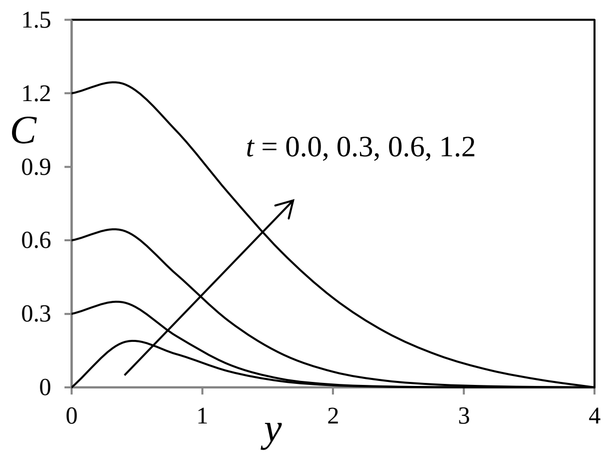

Figure 19. Concentration profiles for different values of time

Figure (15) depicts the effects of the Dufour number on the fluid temperature. It can be clearly seen from this figure that diffusion thermal effects slightly affect the fluid temperature. As the values of the Dufour number increase, the fluid temperature also increases. Figure (16) illustrates the effect of Schmidt number on the concentration field. It is noticed that as the Schmidt number increases, the concentration of the fluid medium decreases significantly in the boundary layer region and thereafter not much of variation is noticed. The effect of Soret number (Sr) on the concentration field is presented in figure (17). From this figure, it is observed that an increase in the Soret number (Sr) leads to increase in the concentration field. Figures (18) and (19) display the effect of the time on temperature and concentration profiles respectively. From these two figures we observe that, both temperature and concentration are increasing with increasing values of time.

The profiles for skin – friction (τ) due to velocity under the effects of Hartmann number, Eckert number, Permeability parameter, Thermal radiation parameter, Heat absorption parameter, Soret number, Dufour number, Chemical reaction parameter, Phase angle and time are presented in the table – 1 respectively.

We observe from this table – 1, the skin – friction rises under the effects of Eckert number, Permeability parameter, Soret number, Dufour number, Thermal radiation parameter and time. And falls under the effects of Hartmann number, Heat absorption parameter, Phase angle and Chemical reaction parameter. The profiles for Nusselt number (Nu) due to temperature profile under the effect of Prandtl number, Eckert number, Thermal radiation parameter, time, Dufour number and Heat absorption parameter are presented in the table – 2. From this table we observe that, the Nusselt number due to temperature profiles rises under the effect of Eckert number, Dufour number, Thermal radiation parameter and time. And temperature profiles falls under the effects of Prandtl number and Heat absorption parameter. The profiles for Sherwood number (Sh) due to concentration profiles under the effect of Schmidt number, Soret number, Chemical reaction parameter and time are presented in the table – 3. We see from this table the Sherwood number due to concentration profiles decreases under the effects of Schmidt number and Chemical reaction parameter and increases with the increasing values of Soret number and time.

Table – 1: Skin – friction results (τ) for the values of M, K, Ec, N, Sr, Du, Q, k_r, α and t

M	K	Ec	N	Q	Sr	Du	k_r	α	t	τ
1.0	1.0	0.0010	1.0	1.0	1.0	1.0	1.0	$\pi/2$	1.0	1.31654894
2.0	1.0	0.0010	1.0	1.0	1.0	1.0	1.0	$\pi/2$	1.0	1.27945621
1.0	2.0	0.0010	1.0	1.0	1.0	1.0	1.0	$\pi/2$	1.0	1.33025491
1.0	1.0	0.1000	1.0	1.0	1.0	1.0	1.0	$\pi/2$	1.0	1.33462159
1.0	1.0	0.0010	2.0	1.0	1.0	1.0	1.0	$\pi/2$	1.0	1.34116954
1.0	1.0	0.0010	1.0	2.0	1.0	1.0	1.0	$\pi/2$	1.0	1.29405618
1.0	1.0	0.0010	1.0	1.0	2.0	1.0	1.0	$\pi/2$	1.0	1.35026459
1.0	1.0	0.0010	1.0	1.0	1.0	2.0	1.0	$\pi/2$	1.0	1.35842165
1.0	1.0	0.0010	1.0	1.0	1.0	1.0	2.0	$\pi/2$	1.0	1.29026489
1.0	1.0	0.0010	1.0	1.0	1.0	1.0	1.0	$2\pi/3$	2.0	1.27036217

Table – 2: Rate of heat transfer (Nu) values for different values of Pr, Ec, N, Q, Du and t

Pr	Ec	N	Q	Du	t	Nu
0.71	0.001	1.0	1.0	1.0	1.0	0.68741184
7.00	0.001	1.0	1.0	1.0	1.0	0.55413624
0.71	0.100	1.0	1.0	1.0	1.0	0.72594875
0.71	0.001	2.0	1.0	1.0	1.0	0.71439985
0.71	0.001	1.0	2.0	1.0	1.0	0.60573605
0.71	0.001	1.0	1.0	2.0	1.0	0.70150548
0.71	0.001	1.0	1.0	1.0	2.0	0.72158491

Table – 3: Rate of mass transfer (Sh) values for different values of Sc, k_r, Sr and t

Sc	k_r	Sr	t	Sh
0.22	1.0	1.0	1.0	1.42916652
0.30	1.0	1.0	1.0	1.32480057
0.22	2.0	1.0	1.0	1.36820629
0.22	1.0	2.0	1.0	1.44571133
0.22	1.0	1.0	2.0	1.45026987

5.Conclusion

We summarize below the following results of physical interest on the velocity, temperature and concentration distributions of the flow field and also on the skin – friction, rate of heat and mass transfer at the wall.

1. A growing Hartmann number or Heat absorption parameter or Chemical reaction parameter or Phase angle retards the velocity of the flow field at all points.
2. The effect of increasing Permeability parameter or Eckert number or Thermal radiation parameter or Soret number or Dufour number or time is to accelerate velocity of the flow field at all points.
3. A growing Prandtl number or Heat absorption parameter decreases temperature of the flow field at all points and increases with increasing of Eckert number or Dufour number or Time or Thermal radiation parameter.
4. The concentration is increases with increasing values of time and Soret number and decreases with increasing of Schmidt number and Chemical reaction parameter.
5. A growing Hartmann number or Heat absorption parameter or Chemical reaction parameter or Phase angle decreases the skin – friction while increasing Permeability parameter or Eckert number or Thermal radiation parameter or Soret number or Dufour number or time increases the skin – friction.
6. The rate of heat transfer is decreasing with increasing of Prandtl number and Heat absorption parameter and increases with increasing of Eckert number, Dufour number, time and Thermal radiation parameter.
7. The rate of mass transfer is decreasing with increasing of Schmidt number and Chemical reaction parameter and increasing of time and Soret number.

References

[1]. Afify, A. A., (2009). Similarity solution in MHD: Effects of thermal diffusion and diffusion thermo on free convective heat and mass transfer over a stretching surface considering suction and injection, *Communications Nonlinear Science and Numerical Simulation*, Vol. 14, pp. 2202 – 2214.

[2]. Alam, S., Rahman, M. M., Maleque A. and Ferdows, M., (2006). Dufour and Soret effects on steady MHD combined free forced convective and mass transfer flow past a semi infinite vertical plate, *Thammasat International Journal Science and Technology*, Vol. 11, No. 2.

[3]. Gaikwad, S. N., Malashetty, M. S. and Prasad, K. R., (2007). An analytical study of linear and non – linear double diffusive convection with Soret and Dufour effects in couple stress fluid, *International Journal of Nonlinear Mechanics*, Vol. 42, pp. 903 – 913.

[4]. Hayat, T., Mustafa, M. and Pop, I., (2009). Heat and mass transfer for Soret and Dufour effects on mixed convection boundary layer flow over a stretching vertical surface in a porous medium filled with a viscoelastic fluid, *Communications in Nonlinear Science and Numerical Simulation* Vol. 15, No. 5, pp. 1183 – 1196.

[5]. Kafoussias, N. G. and Williams, E. W., (1995). Thermal diffusion and Diffusion thermo effects on mixed free forced convective and mass transfer boundary layer flow with temperature dependent viscosity, *International Journal of Engineering Science*, Vol. 33, No. 9, pp. 1369 –1384.

[6]. Lyubimova, T., Shyklyaeva, E., Legros, J, C., Shevtsova, V. and Roux, (2005). Numerical study of high frequency vibration influence on measurement of Soret and diffusion coefficients in low gravity conditions, *Advances in Space Research*, Vol. 36, pp. 70 – 74.

[7]. Mansour, M. A., El – Anssary, N. F. and Aly, A. M., (2008). Effects of chemical reaction and thermal stratification on MHD free convective heat and mass transfer over a vertical stretching surface embedded in a porous media considering Soret and Dufour numbers, *Chemical Engineering Journalf*, Vol. 145, No. 2, pp. 340 – 345.

[8]. Ming – Chun, Li., Yan – wen, T. and Yu – Chun, Z., (2006). Soret and Dufour effects in strongly endothermic chemical reaction system of porous media, *Trans. Non ferrous Met. Soc. China*, Vol. 16, pp. 1200 – 1204.

[9]. Motsa, S. S., (2008). On the onset of convection in a porous layer in the presence of Dufour and Soret effects, *SAMSA Journal of Pure and Applied Mathematics*, Vol. 3, pp. 58 – 65.

[10]. Osalusi, E., Side. and Harris R., (2008). Thermal diffusion and diffusion thermo effects on combined heat and mass transfer of steady MHD convective and slip flow due to a rotating disk with viscous dissipation and Ohmic heating, *International Communications in Heat and Mass Transfer*, Vol. 35, pp. 908 – 915.

[11]. Beg, O. A., Bhargava, R., Rawat, S., Takhar, H. S. and Beg, T. A., (2007). A study of buoyancy – driven dissipative micropolar free convection heat and mass transfer in a Darcian porous medium with chemical reaction, *Nonlinear Analysis: Modeling and Control Journal*, Vol. 12, No. 2, pp. 157 – 180.

[12]. Patil, P. M. and Kulkarni, P. S., (2008). Effects of chemical reaction on free convection flow of a polar fluid through a porous medium in the presence of internal heat generation, *International Journal of Thermal Sciences*, Vol. 47, pp. 1043 – 1053.

[13]. Seddeek, M. A., Darwish, A. A. and Abdelmeguid, M. S., (2007). Effects of chemical reaction and variable viscosity on hydromagnetic mixed convection heat and mass transfer for Hiemenz flow through porous media with radiation, *Communications in Nonlinear Science and Numerical Simulation*, Vol. 12, No. 2, pp. 195 – 213.

[14]. Zueco, J., Beg, O. A., Tasveer, A. and Takhar, H. S., (2008). Numerical study of chemically reactive buoyancy – driven heat and mass transfer across a horizontal cylinder in a non – Darcian porous regime, *Journal Porous Media*.

[15]. Gireesh kumar, J., Satyanarayana, P. V. and Ramakrishna, S., (2009). Effects of chemical reaction and mass transfer on MHD unsteady free convection flow past an infinite vertical plate with constant suction and heat sink, *Journal of Ultra Scientist*, Vol. 21, No. 3, pp. 12 – 28.

[16]. Ibrahim, F. S., Elaiw, A. M. and Bakr, A. A., (2008). Effect of the chemical reaction and radiation absorption on the unsteady MHD free convection flow past a semi infinite vertical permeable moving plate with heat source and suction, *Communications Nonlinear Science Numerical Simulation*, Vol. 13, pp. 1056 – 1066.